Physics Letters B 317 (1993) 631–636
North-Holland

PHYSICS LETTERS B

Test of lepton-flavour conservation in $\mu \rightarrow e$ conversion on titanium

SINDRUM II Collaboration

C. Dohmen, K.-D. Groth, B. Heer, W. Honecker, G. Otter, B. Steinrücken, P. Wintz

III. Physikalisches Institut B der RWTH Aachen, D-52056 Aachen, Germany

V. Djordjadze

High Energy Physics Institute of the Tbilisi State University, 380086 Tbilisi, Georgia

J. Hofmann, T. Kozlowski [1], S. Playfer [2]

Institut für Teilchenphysik der ETH Zürich, CH-5232 Villigen PSI, Switzerland

W. Bertl, J. Egger, W. Herold, B. Krause, H.K. Walter

Paul Scherrer Institut, CH-5232 Villigen PSI, Switzerland

R. Engfer, Ch. Findeisen, M. Grossmann-Handschin [3], E.A. Hermes, F. Muheim [2], C.B. Niebuhr [4], H.S. Pruys, L. Ricken, D. Vermeulen [3] and A. van der Schaaf

Institut für Experimentalphysik der Universität Zürich, CH-8001 Zürich, Switzerland

Received 17 September 1993
Editor: K. Winter

A search for $\mu \rightarrow e$ conversion in muonic atoms is being performed at PSI with the SINDRUM II spectrometer. A first measurement on Ti gives upper limits on the branching ratios for the ground-state transitions of $\Gamma(\mu^- \mathrm{Ti} \rightarrow e^- \mathrm{Ti}^{\mathrm{g.s.}})/\Gamma(\mu^- \mathrm{Ti\ capture}) < 4.3 \times 10^{-12}$ and $\Gamma(\mu^- \mathrm{Ti} \rightarrow e^+ \mathrm{Ca}^{\mathrm{g.s.}})/\Gamma(\mu^- \mathrm{Ti\ capture}) < 4.3 \times 10^{-12}$ (90% confidence). With the assumption of a giant resonance excitation of the Ca nucleus the limit on the total rate for $\mu^- \rightarrow e^+$ conversion is $\Gamma(\mu^- \mathrm{Ti} \rightarrow e^+ \mathrm{Ca}^*)/\Gamma(\mu^- \mathrm{Ti\ capture}) < 8.9 \times 10^{-11}$.

1. Introduction

Experiment puts severe constraints on transitions involving flavour-changing neutral currents, both in the quark and in the lepton sector. Within the framework of the Standard Model they are forbidden at the tree level. The transitions between quarks, such as the recently observed $b \rightarrow s\gamma$ [1], are allowed at the one-loop level via quark mixing. The equivalent lepton-flavour changing transitions, such as $\mu \rightarrow e\gamma$, are strictly forbidden as a consequence of the mass degeneracy of the neutrino states. In most extensions of the Standard Model, however, this selection rule is violated at levels which may be accessible experimentally. The minimal extension, which allows finite neutrino masses, is best tested by measurements of the neutrino mass and by searches for double beta

[1] Permanent address: Institute for Nuclear Studies, PL-05-400 Swierk, Poland.
[2] Present address: Department of Physics, Syracuse University, Syracuse, NY 13244, USA.
[3] Present address: Paul Scherrer Institut, CH-5232 Villigen PSI, Switzerland.
[4] Present address: DESY, Hamburg, Germany.

Table 1
Branching ratios of some muon-number-violating decay modes. All *present* values are upper limits at 90% confidence, with the exception of the Z^0 results, which are given at the 95% confidence level.

Process	Branching ratio	
	present	proposed
$\mu^- \mathrm{Ti} \to e^- \mathrm{Ti}^{g.s.}$	$\leqslant 4.6 \times 10^{-12}$ [4]	3×10^{-14} [5] 10^{-16} [6]
$\mu^- \mathrm{Ti} \to e^+ \mathrm{Ca}^{*}$ a)	$\leqslant 1.7 \times 10^{-10}$ [4]	10^{-12} [5]
$\mu^+ \to e^+ \gamma$	$\leqslant 4.9 \times 10^{-11}$ [7]	6×10^{-13} [8]
$\mu^+ \to e^+ e^+ e^-$	$\leqslant 1.0 \times 10^{-12}$ [9]	
$\mu^+ e^- \leftrightarrow \mu^- e^+$ b)	$\leqslant 6.5 \times 10^{-7}$ [10]	10^{-11} [11]
$\tau^- \to \mu^- \gamma$	$\leqslant 4.2 \times 10^{-6}$ [12]	
$K^+ \to \pi^+ \mu e$	$\leqslant 2.1 \times 10^{-10}$ [13]	5×10^{-12} [14]
$K_L^o \to \mu e$	$\leqslant 3.3 \times 10^{-11}$ [15]	10^{-12} [16]
$Z^0 \to \mu \tau$	$\leqslant 4.8 \times 10^{-5}$ [17]	10^{-6} c)
$Z^0 \to e \mu$	$\leqslant 2.4 \times 10^{-5}$ [17]	10^{-6} c)

a) Assuming a giant resonance excitation with mean energy and width of both 20 MeV.
b) The quoted "branching ratio" is the probability that the system, prepared as $\mu^+ e^-$, is in the $\mu^- e^+$ state by the time of its decay.
c) All LEP experiments.

decay or neutrino oscillations. Most other scenarios, which postulate right-handed currents, additional Higgs bosons, horizontal gauge bosons, leptoquarks, lepton substructure or supersymmetry, are better constrained by the limits on flavour-changing decay modes involving charged leptons; see refs. [2,3] for reviews. Table 1 lists the sensitivities of published and proposed tests of muon-number conservation. Neutrinoless conversion, $\mu^-(A,Z) \to e^-(A,Z)$, in a muonic atom with mass number A and atomic number Z, is one of three classical tests of muon-number conservation; the other two processes are the leptonic decay modes $\mu^+ \to e^+\gamma$ and $\mu^+ \to e^+e^+e^-$. The process $\mu^-(A,Z) \to e^+(A,Z-2)$ violates both muon number and total lepton number. Decays of τ, K and Z^0 also offer possibilities to search for muon-number violation. Which process gives the best constraint is model-dependent, but if muon number is violated the relative rates will help to discriminate between the possible explanations.

When negative muons stop in matter, they form muonic atoms in excited states, which decay electromagnetically to the ground state. The atomic ground state normally decays by muon decay $\mu^- \to e^- \nu_\mu \bar{\nu}_e$ or nuclear muon capture $\mu^-(A,Z) \to (A,Z-1)^* \nu_\mu$. The rate for nuclear capture varies roughly as Z^4 and is larger than the free decay rate of $4.55 \times 10^5\ \mathrm{s}^{-1}$ for $Z > 12$. For Ti the capture probability is 85%.

For $\mu^- \to e^-$ conversion leaving the nucleus in its ground state the transition amplitude, expressed as the sum of the amplitudes for the individual nucleons, has a coherent enhancement unlike transitions to other final states. The dependence of this process on atomic number has been studied by various authors [18–20] In all approaches the branching ratio rises with Z up to a value around $Z = 30$, from where on it remains roughly constant. In the case of $\mu^-(A,Z) \to e^+(A,Z-2)$ there is no coherent enhancement of the ground-state transition [21].

In the process $\mu^-(A,Z) \to e^-(A,Z)^{g.s.}$, the electron is emitted at the kinematical endpoint for bound muon decay; in the case of Ti this is at 104.3 MeV/c. For a momentum resolution better than 2% (FWHM) the background from muon decay occurs at a level below 10^{-14}. Other beam related backgrounds can be induced by pions or electrons contaminating the muon beam. Electron scattering off the target and nuclear π^- capture can be recognised by the occurrence of

a prompt signal in a beam counter. Because of the simple event topology cosmic rays may also produce background.

2. The SINDRUM II experiment

The goal of the SINDRUM II experiment [5] is to search for coherent $\mu \rightarrow e$ conversion with a sensitivity of a few times 10^{-14}. For this purpose a dedicated muon channel will be constructed by the middle of 1995 [22]. This paper describes a first experiment on Ti using an upgraded version of an existing muon channel at PSI. Detailed information on this measurement can be found elsewhere [24–30].

The SINDRUM II spectrometer consists of a superconducting solenoid, which produces a field of 1.2 T in a region of 1.35 m diameter and 1.8 m length, housing the various cylindrical detectors. Charged particles with transverse momenta below 112 MeV/c, which originate in the center of the spectrometer, are confined radially inside the magnet. The detection system is illustrated in fig. 1 , which also shows the tracks of an electron. The innermost detectors at a radius of 28.5 cm are two plexiglas Čerenkov hodoscopes, situated at both ends of the solenoid, with an 80 cm gap between them. The remaining detectors are a 64-element plastic scintillator hodoscope of 3 mm thickness and two drift chambers, DC1 and DC2, covering the radial regions 37.6–44.5 cm and 44.9–65.0 cm respectively. DC1 [23] was filled with CO_2/iC_4H_{10} (70/30), a gas with a low drift velocity which results in a Lorentz deflection of only 6°. DC2 was filled with a He/iC_4H_{10} (88/12) mixture, selected for its large radiation length of 1140 m which results in low multiple scattering. In both chambers the drift field is oriented radially, with the sense wires close to the outer walls. As a result of the energy loss in the scintillating hodoscope the first charge collected on a sense wire originates from the first revolution of the helical trajectory in 99% of the cases. The wall which separates the two drift chambers is made of foam covered by aluminized polyamide foils which serve as cathodes. This wall has a thickness of only 0.8×10^{-3} radiation lengths. The outer cathode of DC1 is subdivided into 4.4 mm wide strips at an angle of 72° relative to the sense wires. Signals from the sense wires and cathode strips from DC1 are assigned to three-dimensional space points on the basis of their strict time correlation.

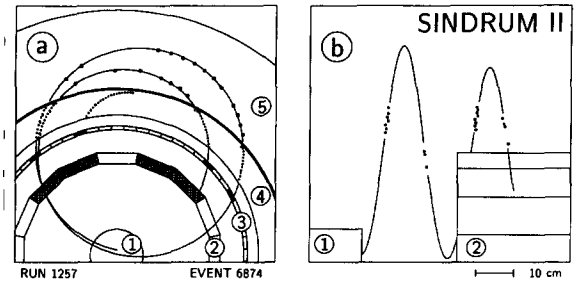

Fig. 1. An electron event in front and side view, (a) and (b), respectively; (1) Ti target, (2) Čerenkov hodoscopes, (3) plastic scintillator hodoscope, (4) drift chamber DC1 and (5) drift chamber DC2. The result of a fit of the electron trajectory to the hits in DC1 is indicated. The reconstructed momentum is 100.6 MeV/c.

The μ^- beam, entering the spectrometer axially, was monitored with a scintillation counter read out with a wave-form digitizer for optimal double-pulse resolution [24]. This information was used to identify prompt background and to determine the number of muons entering the spectrometer. The beam intensity was $1.2 \times 10^7 \mu^-$ s^{-1}, and the e^- and π^- fractions were 5×10^{-2} and 2×10^{-4} respectively. The target was a cylindrical Ti container with a length of 30 cm and a diameter of 14 cm, filled with loosely-packed titanium to give a total mass of 570 g. Outgoing electrons and positrons traversed an unknown amount of target material that varied between 0 and 1 g cm^{-2}. The uncertainty in the energy loss in the target gave the dominant contribution to the momentum resolution. The thickness of a beam moderator was adjusted such that the muon stop distribution peaked at the beginning of the target. Under these conditions 28% of the muons stopped in the target, whereas for pions, which have a shorter mean range, the corresponding fraction was only 2×10^{-4} which led to a pion contamination in the target stops of 1×10^{-7}.

The trigger for data readout accepted both electrons and positrons by requiring two track elements in DC1, at least one hit in the innermost region of DC2 and a Čerenkov signal. The hodoscopes associated with the DC1 tracks were required to be separated by 12–18 modules. The trigger rate was 2 s^{-1} of which half was caused by scattered beam electrons. The resulting data

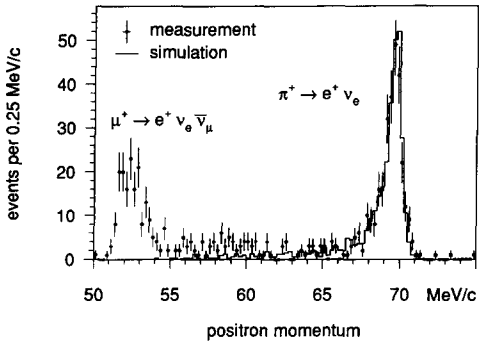

Fig. 2. Positron momentum distribution from the test run with a stopping π^+ beam. The threshold on transverse momentum was just below the endpoint for positrons from μ^+ decay. In the simulated distribution only the decay $\pi^+ \to e^+\nu_e$ was considered.

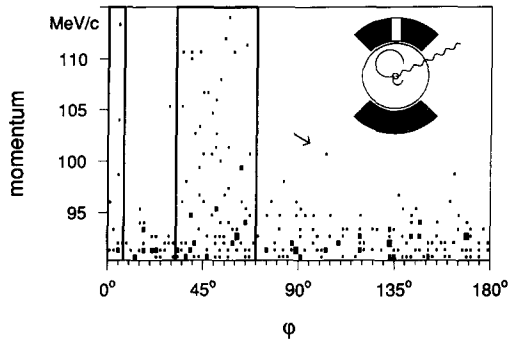

Fig. 3. Distribution of electron and positron momenta versus φ, the emission angle in the plane perpendicular to the symmetry axis of the spectrometer; $\varphi = 0°$ for particles emitted downward. The arrow points at the e^- event shown in fig. 1. The concentration of events in the regions around $\varphi = 0°$ and $\varphi = 45°$ is due to e^+e^- production in the target by photons from cosmic ray showers. The insert illustrates how the return yoke shields partially against this background. The remaining events were removed by the cuts on φ indicated in the figure.

set consists of 3.2 million events collected during a measuring period of 25 days, in which $(4.9 \pm 0.2) \times 10^{12}$ μ^-Ti atoms were formed in the target.

The momenta of the detected electrons and positrons were determined off-line from a fit to the two DC1 tracks from the first turn of the reconstructed trajectory. Lorentz deflection, field inhomogeneities, energy loss and multiple scattering in DC1 and DC2 and energy loss in the hodoscope were taken into account. The signals from DC2 have not been used in the fit, but were taken into consideration in the event reconstruction to help resolve ambiguities and to recognize cosmic ray background. The performance of the spectrometer was studied using 70 MeV/c positrons from the decay $\pi^+ \to e^+\nu_e$. The momentum distribution shown in fig. 2 has a FWHM of 1.5%, in agreement with the expectation from a GEANT [25] simulation. For this measurement a low mass foam target was used to stop a π^+ beam, and the magnetic field was reversed and scaled such that the positron trajectories resembled those expected for conversion electrons as closely as possible.

3. Results

The final analysis is based on the momentum spectra of delayed electrons and positrons originating in the target after suppression of events induced by cosmic rays. Cosmic ray backgrounds were studied during a two week run without beam. Most events could be recognized by the occurrence of additional tracks in the various detectors. One type of cosmic ray event could only be rejected at the cost of a reduction in acceptance. These are asymmetric e^+e^- pairs produced in the target by isolated photons. The events are characterised by pronounced peaks in the angular distribution, shown in fig. 3. The distribution reflects the geometry of the return yoke which shields partially against these photons. The events were removed by limiting the angular acceptance as indicated in fig. 3. Following the measurements reported here a 10 cm thick lead shielding has been mounted to eliminate this problem.

The measured momentum distribution of delayed electrons originating in the target, is compared with distributions from simulations of bound muon decay and coherent $\mu^- \to e^-$ conversion in fig. 4. The event at 100.6 MeV/c is the one which was shown in fig. 1. In the region above 100.6 MeV/c, where 81% of the conversion events are expected, no events were found. The theoretical momentum distribution for bound muon decay resulted from an interpolation of the available calculations for $Z = 18$, 20 and 26 [26]. Radiative corrections led to a rate decrease by about 20% in the region above 70 MeV/c [27]. The contribution from radiative muon capture amounts to 2% for momenta above 70 MeV/c and has been ig-

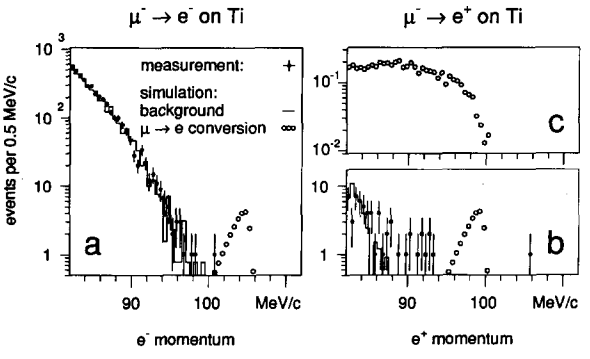

Fig. 4. Momentum distributions for electrons, part a, and positrons, parts b and c, from the decay of μ^-Ti atoms. Distributions from various simulated processes are shown for comparison: bound muon decay and $\mu^-\mathrm{Ti} \to e^-\mathrm{Ti}^{g.s.}$ in part a, radiative muon capture and $\mu^-\mathrm{Ti} \to e^+\mathrm{Ca}^{g.s.}$ in part b, and $\mu^-\mathrm{Ti} \to e^+\mathrm{Ca}^*$ assuming a giant resonance excitation in part c. The simulated spectra for $\mu \to e$ conversion have been normalised under the assumption of a branching ratio of 5×10^{-11}.

nored in the simulation. The agreement between measured and simulated distributions is excellent, both in shape and in total number of events.

The probability for a $\mu^-\mathrm{Ti} \to e^-\mathrm{Ti}$ event to be selected in the final sample, has been determined by simulation,

$$\epsilon_{\mu e} = 0.13 \pm 0.01\,, \tag{1}$$

which can be factorized as

$$\epsilon_{\mu e} = \Omega \times \epsilon_d \times \epsilon_r \times \epsilon_s\,, \tag{2}$$

$\Omega = 0.44$ is the geometric acceptance, $\epsilon_d = 0.68$ is the combined detection and trigger efficiency, $\epsilon_r = 0.83$ is the reconstruction efficiency and $\epsilon_s = 0.52$ is the efficiency associated with the cuts on beam-counter timing, emission angle and total momentum. The branching ratio which would have resulted in one expected event was equal to 1.85×10^{-12}, as determined from $\epsilon_{\mu e}$, the number of muons which stopped in the target during the live time of the experiment and the nuclear capture probability. Since no candidate event was found the measurement resulted in an upper limit at 90% confidence of 2.3 events, which corresponds to

$$\Gamma(\mu^-\mathrm{Ti} \to e^-\mathrm{Ti}^{g.s.})/\Gamma(\mu^-\mathrm{Ti}\ \text{capture}) < 4.3 \times 10^{-12} \quad (90\%\ \text{confidence})\,. \tag{3}$$

The measured positron distribution is shown in fig. 4b. For the transition $\mu^-\mathrm{Ti} \to e^+\mathrm{Ca}^{g.s.}$ the positron momentum varies slightly for the different Ti isotopes. For ^{48}Ti, which has an abundance of 74%, the momentum is 99.0 MeV/c. Since the highest momentum in the region of interest of the measured distribution is 93.5 MeV/c, no candidate events were found for $\mu^-\mathrm{Ti} \to e^+\mathrm{Ca}$ conversion leaving the daughter nucleus in low-lying states. In particular no ground-state transitions have been observed, which in 90% of the events would have resulted in a positron momentum above 93.5 MeV/c. The efficiency for observing a $\mu^-\mathrm{Ti} \to e^+\mathrm{Ca}^{g.s.}$ event in this momentum range was found to be the same as $\epsilon_{\mu e}$, which leads to

$$\Gamma(\mu^-\mathrm{Ti} \to e^+\mathrm{Ca}^{g.s.})/\Gamma(\mu^-\mathrm{Ti}\ \text{capture}) < 4.3 \times 10^{-12} \quad (90\%\ \text{confidence})\,. \tag{4}$$

In earlier searches for $\mu^- \to e^+$ conversion limits on the branching ratio were deduced under the assumption of a giant resonance excitation of the daughter nucleus with a mean excitation energy of 20 MeV and a width of 20 MeV. The expected distribution is shown in fig. 4c. In this case only 5% of the events give a momentum above 93.5 MeV/c and the efficiency is reduced to $\epsilon^*_{\mu e} = 0.0062 \pm 0.0010$. Correspondingly, the upper limit on the branching ratio is raised to

$$\Gamma(\mu^-\mathrm{Ti} \to e^+\mathrm{Ca}^*)/\Gamma(\mu^-\mathrm{Ti}\ \text{capture}) < 8.9 \times 10^{-11} \quad (90\%\ \text{confidence})\,. \tag{5}$$

The dominant source of high-momentum positrons in μ^-Ti decay are asymmetric e^+e^- pairs from radiative muon capture (RMC) with internal or external pair production. Radiative muon decay, which dominates at lower momenta, can be safely ignored. In the RMC simulation the photon spectrum was approximated using the Primakoff formula [33,34], which uses the endpoint energy as a free parameter. Its value was chosen differently for the various isotopes [28]; for ^{48}Ti we used 89.3 MeV as deduced from a measurement of RMC on Ca [29]. The resulting spectrum does not follow the measured distribution in the range between 87 and 94 MeV/c. The extra yield observed here is most likely caused by RMC to low-lying Sc states [4], which is not included in the Primakoff approach.

The upper limits (3)–(5) are slightly lower than those obtained in the most sensitive previous experiment [4]. The results demonstrate the feasibility of the SINDRUM II search which expects to reach a sensitivity of 3×10^{-14} for $\mu^- \to e^-$ conversion within the next few years.

Acknowledgement

The authors wish to thank A. Badertscher, J. Bagaturia, M. Begalli, D. Gähwiler, P. Hawelka, D. Kampmann, N. Khomutov, A. Koller, N. Lordong, G. Melitauri, A. Mtchedlishvili, U. Müller, D. Renker, M. Salzmann, R. Seeliger, G. Souvignier and O. Szavits for their help in the early stages of the experiment. This work was supported in part by the Bundesministerium für Forschung und Technologie, Germany, under contract number 06AC651 and by the Swiss National Science Foundation.

References

[1] CLEO Collab., R. Ammar et al., Phys. Rev. Lett. 71 (1993) 674.
[2] J.D. Vergados, Phys. Rep. 133 (1986) 1.
[3] A. van der Schaaf, in: Progress in particle and nuclear physics, Vol. 31, ed. A. Faessler (Pergamon, Oxford, 1993) p. 1.
[4] S. Ahmad et al., Phys. Rev. D 38 (1988) 2102.
[5] A. van der Schaaf (spokesman), PSI proposal R-87-03 (1987).
[6] R.M. Djilkibaev and V.M. Lobashev (spokesmen), Moscow Meson Factory proposal (1992).
[7] R.D. Bolton et al., Phys. Rev. D 38 (1988) 2077.
[8] M.D. Cooper (spokesman), LAMPF proposal No. 969 (1985).
[9] SINDRUM Collab., U. Bellgardt et al., Nucl. Phys. B 299 (1988) 1.
[10] B.E. Matthias et al., Phys. Rev. Lett. 66 (1991) 2716.
[11] W. Bertl and K. Jungmann (spokesmen), PSI proposal R-89-06 (1990).
[12] CLEO Collab., A. Bean et al., Phys. Rev. Lett. 70 (1993) 138.
[13] A.M. Lee et al., Phys. Rev. Lett. 64 (1990) 165.
[14] M. Zeller (spokesman), BNL proposal E-865 (1990).
[15] K. Arisaka et al., Phys. Rev. Lett. 70 (1993) 1049.
[16] W.R. Molzon, J.L. Ritchie and S.G. Wojcicki (spokesmen), BNL proposal E-871 (1990).
[17] L3 Collab., B. Adeva et al., Phys. Lett. B 271 (1991) 453.
[18] O. Shanker, Phys. Rev. D 20 (1979) 1608.
[19] T.S. Kosmas and J.D. Vergados, Phys. Lett. B 215 (1988) 460.
[20] T.S. Kosmas and J.D. Vergados, Phys. Lett. B 217 (1989) 19.
[21] G.K. Leontaris and J.D. Vergados, Nucl. Phys. B 224 (1983) 137.
[22] C. Niebuhr et al., SINDRUM II Note 16 (1993), unpublished.
[23] M. Grossmann-Handschin et al., Nucl. Instrum. Methods A 327 (1993) 378.
[24] L. Ricken and T. Kozlowski, Nucl. Instrum. Methods A 305 (1991) 232.
[25] R. Brun et al., CERN Report DD/EE/84-1 (1987), unpublished.
[26] F. Herzog and K. Alder, Helv. Phys. Acta 53 (1980) 53.
[27] M. Grossmann-Handschin, Ph.D. thesis, Zürich University, Switzerland (1991), unpublished.
[28] J. Hofmann, Ph.D. thesis, ETH Zürich, Switzerland (1993), unpublished.
[29] M. Doebeli et al., Phys. Rev. C 37 (1988) 1633.